analytical chemistry

Article

pubs.acs.org/ac

Simultaneous Measurement of Individual Mitochondrial Membrane Potential and Electrophoretic Mobility by Capillary Electrophoresis

Gregory G. Wolken and Edgar A. Arriaga*

Department of Chemistry, University of Minnesota, 207 Pleasant Street SE, Minneapolis, Minnesota 55455, United States

Supporting Information

ABSTRACT: Mitochondrial membrane potential varies, depending on energy demand, subcellular location, and morphology and is commonly used as an indicator of mitochondrial functional status. Electrophoretic mobility is a heterogeneous surface property reflective of mitochondrial surface composition and morphology, which could be used as a basis for separation of mitochondrial subpopulations. Since these properties are heterogeneous, methods for their characterization in individual mitochondria are needed to better design and understand electrophoretic separations of subpopulations of mitochondria. Here we report on the first method for simultaneous determination of individual mitochondrial membrane potential and electrophoretic mobility by capillary electrophoresis with laser-induced fluorescence detection (CE-LIF). Mitochondria were isolated from cultured cells, mouse muscle, or liver, and then polarized, labeled with JC-1 (a ratiometric fluorescent probe, which indicates changes in membrane potential), and separated with CE-LIF. Red/green fluorescence intensity ratios from individual mitochondria were used as an indicator of mitochondrial membrane potential. Reproducible distributions of individual mitochondrial membrane potential and electrophoretic mobility were observed. Analysis of polarized and depolarized regions of interest defined using red/green ratios and runs of depolarized controls allowed for the determination of membrane potential and comparison of electrophoretic mobility distributions in preparations containing depolarized mitochondria. Through comparison of these regions of interest, we observed dependence of electrophoretic mobility on membrane potential, with polarized regions of interest displaying decreased electrophoretic mobility. This method could be applied to investigate mitochondrial heterogeneity in aging or disease models where membrane potential is an important factor.

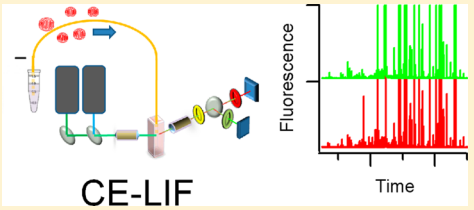

Mitochondrial membrane potential is commonly used as an indication of functional status.[1] Membrane potential arises from a proton gradient established across the mitochondrial inner membrane which drives ATP production through oxidative phosphorylation.[2] While decreased membrane potential (depolarization) indicates damaged, dysfunctional mitochondria that cannot meet cellular energy demands, increased membrane potential (hyperpolarization) leads to increased production of reactive oxygen species, which causes cellular damage, resulting in diseases such as cancer, diabetes, and Alzheimer's.[3] Moreover, changes in mitochondrial membrane potential affect turnover and regulation of dysfunctional mitochondria in the cell through fusion/fission[4] and targeting for elimination by mitophagy (mitochondrial-specific autophagy).[5]

Mitochondrial membrane potential within the cell is heterogeneous and differences in membrane potential can indicate the presence of dysfunctional subpopulations.[6−10] Membrane potential varies according to energy demands, calcium concentrations, and mechanisms to limit reactive oxygen species production in different subcellular locations.[6] Heterogeneity in membrane potential and dysfunctional mitochondria were observed in cells lacking proteins that control mitochondrial morphology (MFN1 and MFN2).[7] In skeletal muscle, subsarcolemmal mitochondria had higher membrane potential than intermyofibrillar mitochondria (two subpopulations characterized by their location).[8] In a cell model of aging, dysfunctional, enlarged mitochondria had lower membrane potential.[9] It was demonstrated that only subpopulations of mitochondria with decreased membrane potential are marked for degradation through mitophagy.[10] In addition to biological sources of heterogeneity, the process of preparing samples of isolated mitochondria itself causes damage to mitochondria, which may result in depolarization and additional apparent heterogeneity in membrane potential.[11]

Methods for measurement of individual mitochondrial membrane potential are needed to characterize mitochondrial heterogeneity and identify subpopulations. Methods using a triphenylphosphonium (TPP^+) ion-selective electrode are quantitative but report only an average value.[12,13] Fluorescent dyes are commonly used in imaging, bulk fluorescence measurements and flow cytometry to indicate mitochondrial membrane potential.[14] These dyes are cationic, which drives their uptake into mitochondria in a membrane potential-dependent manner according to the Nernst equation.[15] JC-1 is one such dye, which is ratiometric, undergoing a spectral shift upon its uptake into mitochondria, which can be measured and used to normalize its response across different dye concentrations or mitochondrial sizes.[14,16−20] The mechanism of

Received: November 27, 2013
Accepted: March 27, 2014
Published: March 27, 2014

   dx.doi.org/10.1021/ac403849x | Anal. Chem. 2014, 86, 4217−4226

spectral change has been established previously and depends on aggregation of JC-1.[21−23] At low concentrations (less than approximately 100 nM), JC-1 exists primarily as a monomer and exhibits green fluorescence.[17] At higher concentrations, JC-1 forms aggregates that exhibit red fluorescence. Mitochondrial membrane potential drives JC-1 uptake into mitochondria; polarized mitochondria with higher membrane potential (more negative with respect to the cytosol) will accumulate JC-1 at a higher concentration than depolarized mitochondria. Polarized mitochondria will therefore exhibit more red fluorescence from aggregates as well as green fluorescence from the monomeric form of the dye, and measurement of red/green fluorescence is then used as an indicator of membrane potential. An advantage for its use in detection of individual mitochondria is that higher dye concentrations result in an increase in signal from red aggregates, as opposed to quenching and reduction of signal seen with other membrane-potential sensitive dyes.[24] JC-1 has been used to measure mitochondrial membrane potential in isolated mitochondria by flow cytometry[25] and in a microfluidic device.[26]

Capillary electrophoresis with laser-induced fluorescence detection (CE-LIF) is a separation technique which has been used for the characterization of mitochondrial heterogeneity.[27] Briefly, isolated mitochondria are labeled with a fluorescent probe or through expression of a fluorescent protein and separated by CE in an aqueous buffer at physiological pH and osmolarity. Individual mitochondrial properties such as DNA content,[28] cardiolipin levels,[29,30] the presence of a specific protein,[31] or the quality of a mitochondrial preparation[32] may be assessed by CE-LIF. This technique can be used for the separation of mitochondrial subpopulations with different surface properties because the electrophoretic mobility of subcellular particles depends on their surface charge density, which is reflective of their surface compositions.[33] Studies on liposomes have revealed that the electrophoretic mobility of biological particles may also depend on properties such as transmembrane pH gradients,[34−37] deformability and field-induced polarization,[35] or multipole effects.[36] Transmembrane pH gradients, which may influence electrophoretic properties through a capacitive effect or by translocation of phospholipids to different sides of the bilayer,[37] are of particular interest in the study of mitochondrial electrophoretic properties since a pH gradient is established across the inner mitochondrial membrane in polarized mitochondria. In previous reports, net mitochondrial mobility has been negative.

Previous work has shown that mitochondrial electrophoretic mobility also depends on membrane potential.[38−40] In these reports, the net mitochondrial mobility was negative. For clarity, when mobilities become less negative, we refer to this change as a decrease in mobility; when mobilities become more negative, we refer to this change as an increase in mobility. Kamo et al. observed increases in mobility of rat liver mitochondria upon polarization using an electric field of 6 V/cm.[38] The authors interpreted this result as an increase in mitochondrial surface charge density and hypothesized that the electrophoretic properties of mitochondria are "affected significantly" by the membrane potential across the inner membrane. In a follow-up study, increases in mitochondrial electrophoretic mobility in a low electric field were again observed upon mitochondrial polarization.[39] The authors suggested that the mitochondrial surface potential at the inner membrane increases with mitochondrial polarization. In another study, increases in mitochondrial mobility and volume upon polarization of rat liver mitochondria was observed with mitochondrial polarization.[40] The authors hypothesized that this result was due to an increase in both mitochondrial surface area and surface charge density and speculated that the outer membrane deforms upon polarization and exposes new charged groups on the surface. While previous studies provided average measurements of mitochondrial electrophoretic mobility or membrane potential, none of them attempted to associate these properties at the individual mitochondrion level.

In this report, we introduce a method to simultaneously measure mitochondrial membrane potential and electrophoretic mobility of individual mitochondria by CE-LIF. Mitochondria were isolated from cultured murine cells, liver, or muscle tissue, energized with succinate in the presence of rotenone (a complex I inhibitor) and then labeled with JC-1. Labeled mitochondria were then separated by CE and detected by a dual-laser excitation/dual-channel emission fluorescence detector. Measurement of red and green fluorescence from JC-1 allowed for determination of individual mitochondrial membrane potential. Valinomycin, an ionophore which allows for free transport of potassium across the mitochondrial inner membrane, was used to depolarize mitochondria as a control.[41] Through comparison of regions of interest containing mitochondrial events considered polarized or depolarized based on their red/green ratios, we observed a dependence of electrophoretic mobility on membrane potential, with higher membrane potential generally resulting in decreases in electrophoretic mobility, which is the opposite trend observed in previous bulk studies. The method described here is useful for investigating mitochondrial heterogeneity and assessment of membrane potential, even if many mitochondria are damaged and depolarized during the preparation and separation, which would not be possible using bulk techniques.

EXPERIMENTAL SECTION

Reagents and Materials. Sucrose, 4-(2-hydroxyethyl)-piperazine-1-ethanesulfonic acid (HEPES), potassium hydroxide (KOH), 5,5′,6,6′-tetrachloro-1,1′,3,3′-tetraethyl-imidacarbocyanine iodide (JC-1), valinomycin, succinic acid, potassium chloride (KCl), magnesium chloride ($MgCl_2$), and poly(vinyl alcohol) (PVA, 99+% hydrolyzed, 89−98 kDa) were from Sigma-Aldrich (Saint Louis, MO). Fluorescein was from Molecular Probes (Eugene, OR). Rotenone was from ICN Biomedicals (Aurora, OH). 5-TAMRA was from AnaSpec (Fremont, CA). Dibasic potassium phosphate (K_2HPO_4) was from Mallinckrodt (Saint Louis, MO). Phosphate-buffered saline (PBS, 10×) was from Bio-Rad (Hercules, CA). Dulbecco's modified Eagle medium (DMEM), fetal bovine serum (FBS), and 0.5% trypsin (10×, 5 g/L trypsin, 2 g/L EDTA·4Na, 8.5 g/L NaCl) were from Gibco (Invitrogen, Carlsbad, CA). Trypan blue stain (0.4%) was from Bio-Whittaker (Walkersville, MD). Fused-silica capillary tubing (50 μm i.d., 150 μm o.d.) was from Polymicro (Phoenix, AZ). Additional reagents and materials are described in the Supporting Information.

Buffers and Solutions. Deionized water was purified using a Synergy filtration system (Millipore, Billerica, MA) and was used in preparation of all buffers and solutions. Intermediate and stock solutions (JC-1, fluorescein, valinomycin, succinate, and rotenone) were prepared as described in the Supporting Information and used at the final concentrations listed in Table 1 below. Buffers were prepared according to Table 1; additional buffers are described in the Supporting Information.

dx.doi.org/10.1021/ac403849x | Anal. Chem. 2014, 86, 4217−4226

Table 1. Buffer Composition[a]

buffer	description	composition
R	respiration buffer, no substrate	125 mM KCl, 10 mM HEPES, 5 mM $MgCl_2$, 2 mM K_2HPO_4
R_s	respiration buffer with substrate	buffer R with 2.5 mM succinate, 2 μM rotenone, 2% DMSO
R_{val}	respiration buffer with substrate and valinomycin	buffer R_s with 2 μM valinomycin
SH	sucrose-HEPES buffer	250 mM sucrose, 10 mM HEPES
SH_s	CE buffer with substrate	buffer SH with 2.5 mM succinate, 2 μM rotenone, 2% DMSO
SH_{val}	CE buffer with substrate and valinomycin	buffer SH_s with 2 μM valinomycin

[a]All buffers were made up in deionized water and adjusted to pH 7.4 with KOH. Buffers were filtered to 0.2 μm before use.

To reduce the fluorescence background for CE-LIF, SH buffer was photobleached using a lab-built device containing 120 blue light-emitting diodes (Super Bright LEDs, Saint Louis, MO) (467 nm, 4.2×10^5 mcd intensity) for at least 24 h before use (see Figure S-1-1 in the Supporting Information). This strategy has been used to reduce the fluorescence background in capillary isoelectric focusing with LIF detection and in single molecule fluorescence experiments.[42,43]

Cell Culture. Adherent C2C12 mouse myoblast and L6 rat myoblast cells (ATCC, Manassas, VA) were cultured in vented 75 cm^2 flasks at 37 °C with 5% CO_2 in DMEM supplemented with 10% FBS. Cells were split after reaching 90% confluence by rinsing with PBS, releasing with 0.25% trypsin in PBS, and seeding back into the flask with fresh DMEM at splitting ratios between 1:20 and 1:40. L6 rat myoblast cells were used for initial experiments, and C2C12 mouse myoblast cells were used in later experiments for a more direct comparison to mouse tissue.

Mitochondrial Preparation and JC-1 Labeling. Mitochondria from cell culture were isolated by differential centrifugation and mechanical homogenization.[44] After isolation, mitochondria were suspended in isolation buffer for cells (buffer C) and kept on ice. Protein content in the mitochondrial fraction was quantified using the Pierce BCA protein assay kit according to the manufacturer's instructions (Thermo, Rockford, IL). Typical mitochondrial protein concentration from one preparation was 1.60 ± 0.09 mg/mL (average ± standard deviation).

Mitochondria were isolated from mouse liver and muscle (hamstring) tissue from C57BL6 mice using published protocols for mechanical homogenization and differential centrifugation.[45] After isolation, liver and muscle mitochondria were resuspended in a minimal amount of isolation buffer for liver or muscle (buffers L and M_2) and kept on ice. Protein concentration (determined using the BCA assay) from this preparation was 23 ± 5 mg/mL for liver mitochondria and 3.2 ± 0.6 mg/mL for muscle mitochondria (average ± standard deviation).

Directly before CE-LIF measurements, aliquots from each isolated mitochondrial fraction (from cells or tissue) were centrifuged and resuspended in buffer R_s containing the substrate succinate and complex I inhibitor rotenone (or buffer R_{val} for depolarized controls, containing the potassium ionophore valinomycin in addition to the substrate and inhibitor). The mitochondria were incubated in the dark for 10 min at 37 °C with 300 rpm mixing in an Eppendorf Thermomixer (Hamburg, Germany). JC-1 was then added to a final concentration of 1 μM, and the samples were incubated for an additional 10 min at 37 °C. Mitochondria were then kept at room temperature in the dark and analyzed by CE-LIF or in the plate reader. For subsequent CE-LIF runs, new aliquots from the original mitochondrial fraction were centrifuged, resuspended in buffer R_s (or buffer R_{val} for depolarized controls), and labeled with JC-1 directly before analysis. This procedure decreases loss of JC-1 over time due to consumption of substrate that results in loss of membrane potential (see Figure S-1-2 of the Supporting Information).[14]

Bulk Measurement of JC-1 Fluorescence. Bulk red and green fluorescence from mitochondrial samples labeled with JC-1 was measured with a BioTek Synergy 2 well plate reader (Winooski, VT) in 96-well plates (Nunc, Roskilde, Denmark). Red (λ_{ex} = 530 ± 12.5 nm, λ_{em} = 590 ± 17.5 nm) and green (λ_{ex} = 485 ± 10 nm, λ_{em} = 528 ± 10 nm) fluorescence was acquired using the auto sensitivity mode, and red/green ratios were calculated to indicate the mitochondrial membrane potential. Controls (buffer R and buffer R containing JC-1 at the same concentration used for labeling mitochondria) were included (see Figure S-1-3 of the Supporting Information).

Validation of JC-1 as a Ratiometric Probe for Membrane Potential. Confocal fluorescence microscopy and membrane potential measurement with a TPP^+ ion-selective electrode[12] were performed to validate the response of JC-1 to changes in membrane potential in intact cells and isolated mitochondria. See Figures S-1-4 and S-1-5 of the Supporting Information for details.

Instrument Description. A home-built capillary electrophoresis instrument which has been described previously[46] has been adapted for this work. For more efficient excitation of JC-1, a 5 mW HeNe laser (Melles-Griot, Carlsbad, CA) was added to the instrument. The 543.5 nm light from this laser was combined with the 488 nm light from a 12 mW Ar^+ laser (Melles-Griot, Carlsbad, CA) using a 503 nm dichroic beam combiner (Semrock LM01-503-25, Rochester, NY) and was focused through the sheath-flow cuvette for postcapillary detection. Light was collected at 90° to the lasers by a 40×, 0.55 NA objective (New Focus, San Jose, CA). Scattered laser light was eliminated with a 488/543 nm dual notch filter (NF01-488/543-25, Semrock). Fluorescence was passed through a pinhole, split into red and green channels using a 540 nm long-pass dichroic mirror (XF2013, Omega Optical, Brattleboro, VT), and passed through a 593 ± 20 nm (red channel) or 520 ± 17.5 nm (green channel) band-pass filter (BrightLine Fluorescence Emitter, Semrock) onto photomultiplier tubes (PMT, R1477, Hamamatsu) biased at 1000 V. See Figure S-1-6 of the Supporting Information for transmission spectra of the filter set used in the CE-LIF detector.

Capillary Preparation. To reduce mitochondrial adsorption to the capillary surface,[47] fused-silica capillaries were permanently coated with adsorbed PVA by a method adapted from Shen et al. (see Section S.5 of the Supporting Information).[48] The PVA-coated capillary was trimmed to ~40 cm, installed in the instrument, and initially aligned by flushing a solution of 5×10^{-9} M fluorescein and 5×10^{-8} M 5-TAMRA in the SH buffer by application of pressure to the inlet. These two fluorophores were selected as they are compatible with the dual-laser excitation/dual channel fluorescence emission detection system (fluorescein is excited by the 488 nm laser and detected in the green channel; 5-TAMRA is excited by the 543.5 nm laser and detected in the red channel).

dx.doi.org/10.1021/ac403849x | Anal. Chem. 2014, 86, 4217−4226

For fine alignment of the capillary, a solution of 2.5 μm Alignflow flow cytometry beads for 488 nm excitation (Invitrogen) in SH buffer was continuously injected by application of an electric field of −400 V/cm with the PMTs biased at 300 V. Alignment was considered acceptable when the relative standard deviation of the average fluorescence intensity from each bead event in the red channel was less than 20% (see Figure S-1-7 of the Supporting Information).

CE Procedure. The capillary was rinsed with buffer SH_s directly before the CE-LIF runs or with buffer SH_{val} before runs of depolarized controls. Mitochondrial samples were diluted with buffer SH_s (or buffer SH_{val} for depolarized controls), and fluorescein was added to a final concentration of 5×10^{-10} M. Fluorescein was used as an internal standard to calculate the limit of detection and electroosmotic flow (EOF). Typical mitochondrial protein content of injected samples, as determined by the BCA protein assay, was 1.5 ng for liver mitochondria, 1.0 ng for muscle mitochondria, and 0.25 ng for mitochondria from cultured cells, although it was necessary to use trial and error to find a dilution factor that resulted in an acceptable number of mitochondrial events (see the discussion of peak overlap of the Supporting Information). Samples were injected hydrodynamically by siphoning; an electronically actuated valve (Parker Hannifin, Cleveland, OH) was used to increase the height difference between the inlet of the capillary and the sheath flow waste to 110 cm for 2.7 s. After injection, the inlet of the capillary was rinsed twice in SH buffer and switched to the vial of running buffer (buffer SH_s or SH_{val} for depolarized controls). An electric field of −400 V/cm was applied for 15 min for the CE separation. Between runs, the capillary was rinsed with DMSO for 5 min and fresh running buffer for 5 min. The peak height and migration time of fluorescein were used to calculate the limit of detection and EOF, respectively. For a typical experiment, the limit of detection ($S/N = 3$) was 26 ± 1 zmol, and the EOF was 9.4 ± 0.1 × 10^{-5} cm^2 V^{-1} s^{-1} ($n = 7$). This reduction in EOF from a previously reported value for uncoated fused silica of 5.1 ± 0.1 × 10^{-4} cm^2 V^{-1} s^{-1} indicates a successful PVA coating.[49]

Data Analysis. Data from the PMTs was acquired at 200 Hz, digitized by an I/O data acquisition card (PCIMIO-16E-50) operated by Labview 5.1 (National Instruments) and stored as a binary file. Data were analyzed in Igor Pro (Wavemetrics, Lake Oswego, OR) by a procedure written in-house which has been described previously, PeakPicks.[50] Briefly, electropherograms were median-filtered to separate narrow spikes (with baseline widths below 200 data points or 1.0 s) from broad peaks (such as fluorescein). Spikes with signal intensity above a threshold of 5 standard deviations over the background signal were assigned to mitochondrial events. Coincident events (events with maxima in both red and green channels at the same migration time, with a tolerance of 0.01 s) were then selected. The electrophoretic mobility and corrected electrophoretic mobility (electrophoretic mobility minus the mobility of the EOF) was calculated for each mitochondrial event based on its migration time.

Two potential issues in organelle analysis by CE-LIF are detection of false positives and peak overlap. The first issue was evaluated by performing a blank injection and by counting the number of events in a premigration window in each run.[27] The relevance of the second issue was assessed with statistical overlap theory.[51,52] None of these two issues posed significant problems (see Figure S-1-8, Table S-1-2, and Table S-1-3 of the Supporting Information for details).

Polarized and depolarized regions of interest (ROIs) containing mitochondrial events considered polarized or depolarized based on their red/green ratios were defined in each CE-LIF experiment. A similar graphical approach has been used previously to define groups of polystyrene microspheres with distinct fluorescence and scattering properties analyzed by CE-LIF.[53] First, red versus green fluorescence intensities of each coincident event were plotted for samples and depolarized controls of each type (cells, muscle, and liver). A line drawn from the origin was used to divide the data into polarized and depolarized ROIs (i.e., with the polarized ROI located above the line and the depolarized ROI below it). To verify that a linear definition of ROIs is valid, various least-squares fits (e.g., linear, polynomial, exponential) were performed on the data; the nonlinear fits were not significantly better than the linear fit (see Table S-1-4 of the Supporting Information). The slope of the line was then varied to maximize the percentage of events in the polarized ROI from each sample compared to the percentage events in the polarized ROI from the depolarized control (see Figure S-1-9 of the Supporting Information). Results of this ROI analysis are shown in Figure S-1-10 and Table S-1-5 of the Supporting Information and discussed below.

RESULTS AND DISCUSSION

Validation of JC-1 as Membrane Potential Indicator. We validated the sample preparation procedure by measuring the average membrane potentials of an isolated mitochondrial sample and its depolarized control (2 μM valinomycin) using a TPP^+ ion-selective electrode (see Figure S-1-5 of the Supporting Information). Membrane potential was calculated as −125 and −80 mV for the mitochondrial sample and depolarized control, respectively. These values are comparable to values previously determined by this technique: mitochondria isolated from rat liver and energized with succinate were reported to have a membrane potential of −172 mV, which dropped to around −110 mV (value estimated from the reported data) upon depolarization with FCCP.[12] While an advantage of this technique over the measurement of bulk JC-1 fluorescence is the ability to calculate numeric values of membrane potential, it is not suitable for analysis of individual mitochondria or subpopulations because it reports an average value.

We evaluated the suitability of the membrane potential dyes TMRM, R123, and JC-1 for use in isolated mitochondria since the free dye must be removed from the medium prior to CE-LIF analysis (see Figure S-2-1 of the Supporting Information). Unlike the fluorescence intensity of TMRM or rhodamine 123 that decreases upon dye removal, JC-1 red/green ratio in isolated mitochondria was similar before and after the free dye was removed from the medium, indicating its suitability for use in CE-LIF.

We confirmed that JC-1 responds to changes in mitochondrial membrane potential in cultured cells by observation of L6 rat myoblasts and depolarized control cells (2 μM valinomycin) with confocal fluorescence microscopy (see Figure S-1-4 of the Supporting Information). Indeed, cells exhibit intense red fluorescence from JC-1 aggregates, and depolarized control cells exhibit very weak red fluorescence and more intense green fluorescence from JC-1 monomers. While imaging is a useful technique for observing mitochondrial membrane potential heterogeneity and provides the advantage of observations of mitochondrial morphology,[6] this technique is not suitable for

measurement of electrophoretic mobility, which can provide information about surface properties of mitochondria which could be used to separate subpopulations. Additionally, without automation of image collection and data analysis, characterization of large numbers of mitochondria is time-consuming. Another potential issue when measuring mitochondrial membrane potential in intact cells (as opposed to using isolated mitochondria) is that JC-1 equilibration may depend on mitochondrial morphology.[14]

In bulk measurements done on a well plate reader, we also investigated the response of JC-1 fluorescence to depolarization in isolated mitochondria from cultured L6 rat myoblasts, C2C12 mouse myoblasts, and mouse liver and muscle tissue. In initial control experiments, we determined that the presence of the protonophore CCCP, commonly used to depolarize mitochondria, reduced the measured red/green fluorescence of JC-1 in free solution. In contrast, valinomycin did not change the observed red/green ratio of different concentrations of free JC-1 (see Figure S-2-2 of the Supporting Information). Similar results were obtained in isolated mitochondria from all sources (i.e., mitochondria exhibit more intense red fluorescence and higher red/green ratios than depolarized controls). Thus, valinomycin was used to depolarize mitochondria used in CE-LIF measurements described below.

CE-LIF. Individual mitochondrial events were detected in CE-LIF separations (see Figure 1). Red and green fluorescence from mitochondria labeled with JC-1 was observed using this technique, similar to the two color-measurements obtained in microscopy and bulk fluorescence methods (see Section S.3 of the Supporting Information).

The run-to-run reproducibility of CE-LIF measurements was evaluated by performing three replicate injections of mitochondria and of depolarized control mitochondria isolated from a C2C12 mouse myoblast preparation. Data from individual runs (see Figure S-2-3 of the Supporting Information) are combined to show overall distributions of red/green ratio (Figure 2 A)

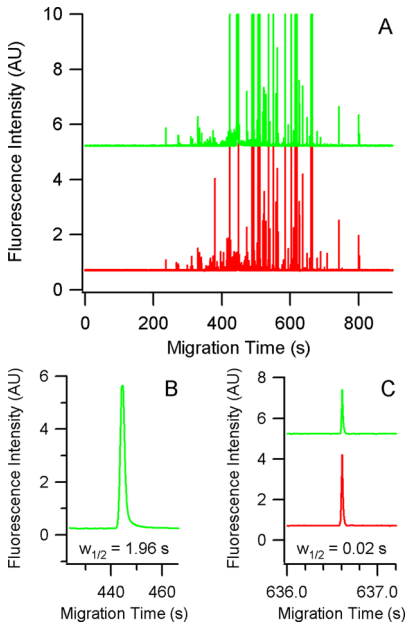

Figure 1. CE-LIF trace of JC-1 labeled mitochondria from muscle tissue. (A) Electropherograms, bottom and top traces show JC-1 fluorescence in red (593 ± 20 nm) and green (520 ± 17.5 nm) channels, respectively. Y-offset is +5 for the green channel. (B) Fluorescein peak in green channel after median filtering to separate spikes from wide peaks. (C) Mitochondrial event in red and green channels. Y-offset is +5 for green channel. Samples were hydrodynamically injected by creating a height difference of 110 cm between inlet and outlet for 2.7 s. Separations were performed in a 50 μm i.d. fused silica capillary coated with PVA at −400 V/cm in buffer SH_s or SH_{val} for runs of depolarized controls.

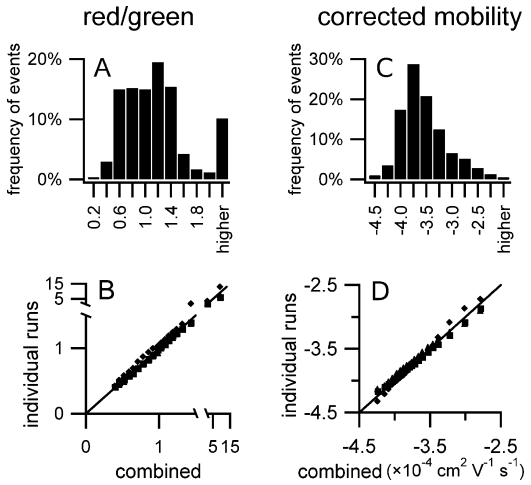

Figure 2. Reproducibility in multiple CE-LIF runs of mitochondria isolated from C2C12 cells. (A) Distribution of red/green ratios from three combined replicate runs, n = 950 detected events. (B) Q−Q plot of red/green ratios from individual runs vs combined data. (C) Distribution of corrected electrophoretic mobility from the three combined runs. (D) Q−Q plot of corrected mobility from individual runs vs combined data. See Figure S-2-3 of the Supporting Information for the distributions of individual runs, Figures S-2-4 and S-2-5 of the Supporting Information for data from depolarized controls, and Table S-2-1 for the normalized ss_{res} for Q−Q plots of the Supporting Information. CE-LIF conditions as described in Figure 1.

and corrected electrophoretic mobility (Figure 2C). Individual and combined distributions from runs of depolarized controls are shown in Figures S-2-4 and S-2-5 of the Supporting Information.

Overall, the distributions of red/green ratios and corrected electrophoretic mobility were reproducible. This is demonstrated by comparisons of individual runs to the data from all combined runs using quantile−quantile (Q−Q) plots, which have been used to compare mitochondrial mobility distributions in capillary electrophoresis.[54] In this approach, the 5th through 95th percentiles of two data sets are plotted against one another; identical distributions would produce plots with points that fall on a line defined by $y = x$. We determined the normalized sum of squares of residuals (ss_{res}) for quantitative comparisons of data from Q−Q plots.[49] The normalized ss_{res} is given by eq 1, where the median is from the data plotted on the x axis.

$$\text{normalized} ss_{res} = \frac{\sqrt{ss_{res}}}{\text{median}} \times 100\% \quad (1)$$

The normalized ss_{res} is similar to the relative standard deviation of a data set, and larger values indicate less similar distributions. Distributions of red/green ratio and corrected electrophoretic mobility were consistent from run to run; the Q−Q plots (Figure 2, panels B and D) show data points from individual runs falling close to the $y = x$ line. The 5th−85th

dx.doi.org/10.1021/ac403849x | Anal. Chem. 2014, 86, 4217−4226

percentiles for red/green ratio distributions were reproducible (normalized ss_{res} = 26%, 18%, and 13% for runs 1, 2, and 3, respectively). The larger normalized ss_{res} for the 90th−95th percentiles reflects the higher and more variable red/green ratios in these percentiles. Distributions of corrected electrophoretic mobility were also reproducible, with normalized ss_{res} = 7%, 7%, and 5% for runs 1, 2, and 3, respectively.

CE-LIF versus Bulk Measurement of JC-1 Fluorescence. While bulk measurements done on a well-plate reader show clear changes in the red/green ratio upon depolarization of mitochondrial samples, median values from the overall distributions of red/green ratios of JC-1 fluorescence of individual mitochondrial events detected by CE-LIF did not follow the same trend (Figure 3). For the mitochondrial

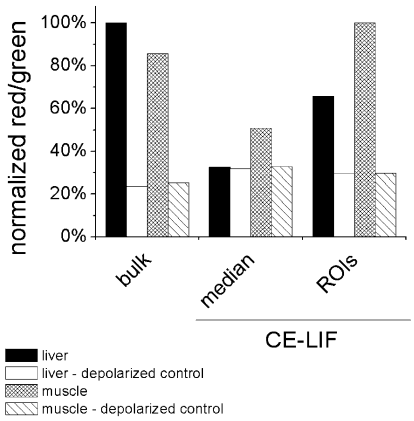

Figure 3. Comparison of red/green ratios from bulk measurements to median values and ROIs from CE-LIF. Mitochondria were isolated from mouse liver and muscle tissue. All bulk measurements are normalized to the highest red/green ratio among bulk measurements; all CE-LIF median values are normalized to the highest median value among CE-LIF groups (i.e., the polarized ROI from the muscle sample). Bulk red fluorescence: λ_{ex} = 530 ± 12.5 nm and λ_{em} = 590 ± 17.5 nm. Bulk green fluorescence: λ_{ex} = 485 ± 10 nm and λ_{em} = 528 ± 10 nm. CE-LIF conditions are the same as in Figure 1.

samples and their respective depolarized controls, the median red/green ratios of individual mitochondrial events detected by CE-LIF did not change. Three reasons may account for these differences. First, in the bulk technique, red or green fluorescence is the sum of fluorescence from mitochondria containing JC-1 and from all JC-1 in free solution; in the LIF measurements, free JC-1 is not detected because it migrates away from the detector (see Figure S-1-8 of the Supporting Information). This could result in an overestimation of the red/green ratio in bulk because red JC-1 aggregates are present in free solution at the labeling concentration used. Second, JC-1 response in bulk is known to depend on mitochondrial concentration.[20] Indeed, when mitochondria labeled with JC-1 were diluted to lower concentrations, we observed decreases in the bulk red/green ratio (see Figure S-2-7 of the Supporting Information). Dilution to the individual mitochondrial level is therefore expected to result in low red/green ratios, which makes it difficult to observe changes due to depolarization. Third, the bulk fluorescence technique may not be sensitive to the presence of depolarized mitochondria in a preparation. Depolarized mitochondria result from experimental factors such as damage during mechanical homogenization or loss of membrane potential over time after isolation. We anticipate having depolarized mitochondria in the preparation used here because we used mechanical homogenization, which is a harsh cell disruption procedure,[11] and vortexing at 300 rpm to mix isolated mitochondria with JC-1 during labeling. In addition, isolated mitochondria lose membrane potential over time (see Figure S-2 of the Supporting Information), increasing the number of depolarized mitochondria in the sample. The red/green ratio will not change dramatically as mitochondria depolarize because JC-1 aggregates will slowly dissociate, while total concentration of the JC-1 monomer will remain constant.

Region of Interest (ROI) Analysis. Similar to bulk measurements, the median values of red/green ratios from CE-LIF data do not represent the effect of depolarization on entire distributions of red/green ratios of individual mitochondrial events. To address this issue, we defined polarized and depolarized ROIs based on the red/green ratios of individual mitochondrial events detected in samples and depolarized controls (Figure 4). This approach addresses the issue that l mitochondrial preparations always include a fraction of depolarized mitochondria that will affect the observed membrane potential.

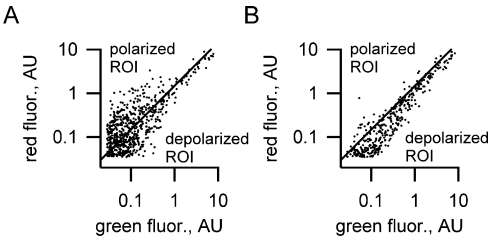

Figure 4. Definition of ROIs in CE-LIF. (A) Mitochondrial events from muscle sample with ROIs shown. (B) Mitochondrial events from depolarized control with ROIs shown. CE-LIF conditions as in Figure 1. Plots with a linear scale are shown in Figure S-1-10 of the Supporting Information.

To define the ROIs, the slope of a line defining the polarized and depolarized ROIs was varied to maximize the difference in the percentage of events in the polarized ROI between samples and depolarized controls (see Figure S-1-9 and Table S-1-5 of the Supporting Information). The polarized ROIs contained 53%, 49%, and 18% of the total events in samples from cells, muscle, and liver, respectively. The median red/green ratios in the depolarized ROI from samples and depolarized controls are similar (see Figure 3), which supports this approach to define ROIs. This approach allows for the comparison of subpopulations of polarized and depolarized mitochondria within a single sample.

In theory, the sample and depolarized control should display mitochondrial events only in the polarized and depolarized ROIs of their respective plots. As discussed above (see subsection, CE-LIF versus Bulk Measurement of JC-1 Fluorescence), polarized mitochondrial samples have depolarized mitochondria, which is in agreement with the presence of individual mitochondrial events in the depolarized ROI (Figure 4A).

In contrast, we did not anticipate finding mitochondrial events within the polarized ROI for depolarized samples. Three possible explanations are false positives, detector cross-talking, and the presence of mitochondria resistant to depolarization. First, some of these events are false positives resulting from the

dx.doi.org/10.1021/ac403849x | Anal. Chem. 2014, 86, 4217−4226

empirical approach to define ROIs. Second, cross-talking in the flow cytometric analysis of mitochondria labeled with JC-1 has been reported previously.[55] In this report the broad fluorescence emission peak from the monomer would also be detected in the detector channel used to measure the fluorescence of JC-1 aggregates (593/40 nm bandpass filter; see Figure S-1-6 of the Supporting Information). We estimate that there is a 10% cross-talk, which may contribute to assigning a higher red/green ratio to some depolarized mitochondria. Lastly, some mitochondria may not be fully depolarized. Others have reported that some preparations have a small fraction of isolated mitochondria that are resistant to depolarization upon treatment with FCCP.[56] They suggested that this phenomenon results from having variations in inner membrane composition, which would affect transport of the depolarizing agents.

The advantages of CE-LIF over bulk techniques are that red/green fluorescence intensity ratios and electrophoretic mobility data are collected from hundreds of individual mitochondria in a single 15 min run, allowing for determination of individual mitochondrial membrane potential and investigation of mitochondrial heterogeneity in membrane potential and surface properties. Most importantly, detection of individual mitochondria and the definition of polarized and depolarized ROIs make it possible to investigate mitochondrial membrane potential heterogeneity in CE-LIF runs containing both polarized and depolarized mitochondria.

The use of ROIs made comparisons possible between the medians of the red/green ratios of mitochondrial events in polarized and depolarized ROIs with the bulk measurements (see Figure 3). The red/green ratios defined by ROIs parallel those observed in bulk measurements. It is worth mentioning that the time spanned between sample preparation and analysis varied for the muscle and liver sample, which implies that there are different fractions of depolarized mitochondria in each preparation (Figure S-1-2 of the Supporting Information indicates that some depolarization does occur over this time frame). The median of the red/green ratios for muscle mitochondria is higher than that of liver mitochondria, which is in agreement with the longer time elapsed between preparation and analysis of liver mitochondria. Together, these results demonstrate the need for the use of polarized and depolarized ROIs for comparison of mitochondrial membrane potentials determined by CE-LIF with bulk measurements.

The definition of ROIs is important for comparing distributions of individual polarized and depolarized mitochondria. The comparison of the red/green ratios in polarized and depolarized ROIs (histograms in Figure 5A) shows a large deviation of the data from the $y = x$ line in Figure 5B (white ○), which demonstrates the difference between the two distributions. The histograms (Figure S-2-8 of the Supporting Information) and Q−Q plots (Figure 5 B, solid dots) of red/green ratio of overall distributions illustrate little difference between the sample and depolarized control (i.e., data points do not deviate much from the $y = x$ line shown on the plot in Figure 5B, normalized ss_{res} = 24% for the 5th−85th percentiles).

Dependence of Electrophoretic Mobility on Membrane Potential. In this study, we calculated the electrophoretic mobility for each individual mitochondrial event detected by CE-LIF. There is only a slight difference in the overall distributions of corrected electrophoretic mobility (Figure S-2-9 of the Supporting Information) between the

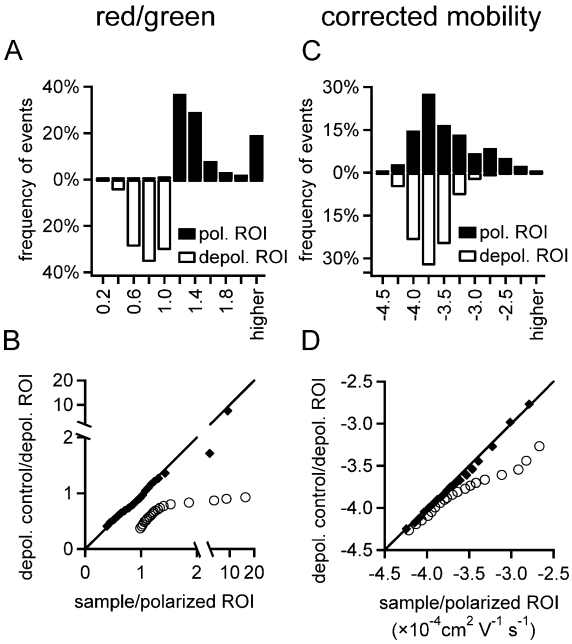

Figure 5. Comparison of polarized vs depolarized ROIs using mitochondria isolated from C2C12 cells. (A) Histograms of red/green ratio distributions of polarized ROI from samples and depolarized ROI from depolarized controls. Polarized ROI: n = 501 events, 3 runs. Depolarized ROI: n = 503 events, 3 runs. (B) Q−Q plot of red/green ratio comparing overall distributions of depolarized controls vs samples (◆) and depolarized vs polarized ROIs (○). (C) Histograms of corrected electrophoretic mobility distributions of polarized ROI from samples and depolarized ROI from depolarized controls. (D) Q−Q plot of corrected electrophoretic mobility comparing overall distributions of depolarized controls vs samples (◆) and depolarized vs polarized ROIs (○). See Figures S-2-8 and S-2-9 of the Supporting Information for the histograms of the overall distributions and Table S-2-1 for the normalized ss_{res} for Q−Q plots of the Supporting Information. CE-LIF conditions are the same as in Figure 1.

sample and the depolarized control, with the depolarized control distribution being slightly more positive than the sample distribution (Q−Q plot in Figure 5D solid dots, normalized ss_{res} = 6%). In order to assess differences between the electrophoretic mobilities of polarized and depolarized mitochondria, we determined the differences in corrected electrophoretic mobility distributions between polarized and depolarized ROIs (Figure 5, panels C and D, white ○). The comparison showed that there are clear differences in electrophoretic mobilities between polarized and depolarized mitochondrial events, with increasing differences in percentiles above the 50th percentile (normalized ss_{res} = 37%).

Previous studies, reported that polarization of mitochondria resulted in an increase in electrophoretic mobility (more negative), which was attributed to increased mitochondrial surface charge density.[38−40] The results obtained here indicate the opposite trend. We observed that polarized mitochondria had lower electrophoretic mobilities than those of depolarized mitochondria. A key difference between previous studies was that they used low electric fields (e.g., 6 V/cm),[38−40] while we used a relatively higher electric field in this study (i.e., −400 V/cm). At these higher field strengths, the electrophoretic mobility of biological "soft" particles is decreased by factors such as deformability, field-induced polarization, the relaxation effect, and multipole moments,[35] which are not as apparent at

dx.doi.org/10.1021/ac403849x | Anal. Chem. 2014, 86, 4217−4226

the lower electric field strengths (e.g., 6 V/cm) used in previous electrophoretic studies of mitochondria.[38−40] In agreement, the effect of electric fields on the electrophoretic mobilities of mitochondria determined by CE-LIF using an electric field of −360 V/cm were lower by 1.8×10^{-4} cm^2 V^{-1} s^{-1} than those determined by free-flow electrophoresis using an electric field of −14.3 V/cm.[44] The relaxation effect was thought to cause the observed difference in electric-field-dependent electrophoretic mobilities.[33]

At the high electric field used here, differences in electrophoretic mobilities between polarized and depolarized mitochondria may be associated with chemical gradients across the mitochondrial inner membrane. Studies done on the electrophoretic mobilities of liposomes with a pH gradient (proton gradient) across their membrane may be relevant to explain the connections between membrane potential (chemical gradient) and their electrophoretic mobilities. A pH gradient across the liposomal membrane can influence surface charge through a capacitive effect, where an excess of negative charge on one side of the membrane increases the positive charge on the other side.[34,37] Liposomes with an internal pH of 8.8 suspended in a biological buffer at 7.4 are comparable to polarized mitochondria, which are expected to have a higher internal pH and a net negative charge on the inner side of the inner membrane. Liposomes with an internal pH of 7.4 suspended in a biological buffer at the same pH resemble depolarized mitochondria. In agreement with a capacitive effect (excess of negative charge inside), liposomes with a pH gradient have lower electrophoretic mobility than that of liposomes without a pH gradient.[34−37] Thus, the capacitive model is a plausible explanation for the electrophoretic mobility differences associated with polarized and depolarized mitochondria reported here.

Besides the capacitive effect, other factors may contribute to the observed differences in electrophoretic mobility between polarized and depolarized mitochondria. For instance, the capacitive model would account for a gradient across the mitochondrial inner membrane, but does not describe the contribution of the mitochondria outer membrane, which also has electrical charges, but it is permeable to low molecular weight species.[57] Although future studies are needed to establish a relationship between membrane potential and electrophoretic mobility, our method represents an important tool for studying this relationship, even in samples containing depolarized mitochondria due to its ability to characterize the membrane potential and electrophoretic mobility of individual mitochondria.

Application to Liver and Muscle Tissue Mitochondria. Use of ROIs allows for characterization of tissue-specific mitochondrial mobility and membrane potential not seen in their respective overall distributions of individual data. The distributions of the red/green ratio and corrected electrophoretic mobility from mitochondrial samples and depolarized controls isolated from mouse muscle and liver tissue are shown in Figure 6. In mitochondria from muscle, differences in the red/green ratio distributions between samples and depolarized controls were apparent even in the overall data (shown in Figure S-2-10 of the Supporting Information), and were more pronounced in the ROI comparison (Figure 6A). Differences in the distributions of red/green ratio from liver mitochondria were less pronounced between samples and depolarized controls when considering the overall distributions. The difference in the distributions from polarized and depolarized

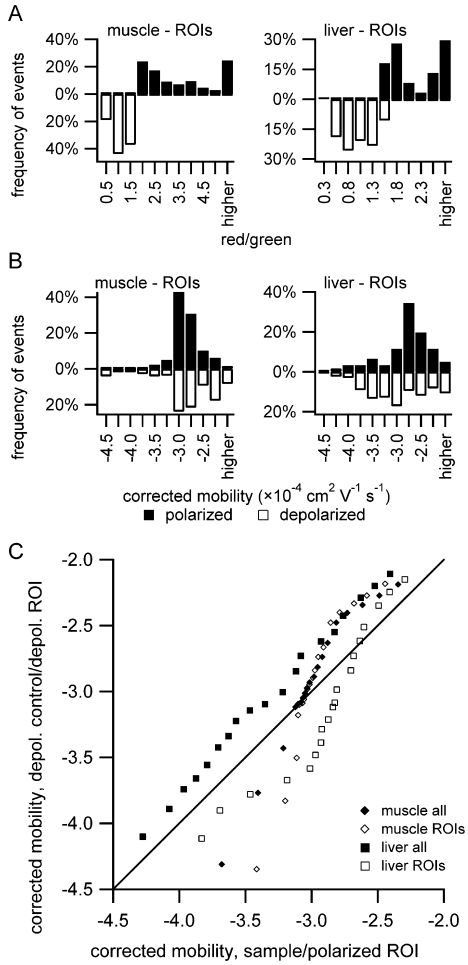

Figure 6. CE-LIF of muscle and liver tissue mitochondria. (A) Distributions of red/green ratio from polarized and depolarized ROIs. (B) Distributions of corrected electrophoretic mobility from polarized and depolarized ROIs. (C) Q−Q plots of corrected electrophoretic mobility ($\times 10^{-4}$ cm^2 V^{-1} s^{-1}). Comparisons are made between samples and depolarized controls (all events) and between events in polarized ROIs and depolarized ROIs. See Figures S-2-10 and S-2-11 of the Supporting Information for histograms of the overall data and Q−Q plot of red/green ratios, Table S-1-5 for number of events, and Table S-2-1 for normalized ss_{res} from Q−Q plots. CE-LIF conditions are the same as in Figure 1.

ROIs was much more pronounced, illustrating the value of measuring individual mitochondrial membrane potential. As discussed previously, the smaller red/green ratios from liver mitochondria could reflect mitochondrial degradation due to the sample preparation procedure or loss of membrane potential over time, as these samples were analyzed after the muscle samples. Detection of smaller red/green ratios in the liver sample supports the utility of defining a polarized ROI: as more mitochondria lose membrane potential over time, our method is still adequate to assess the polarization states of mitochondria by examining ROIs.

Differences in distributions of corrected electrophoretic mobility (Figure 6, panels B−C) are similar to those observed in the experiments with mitochondria isolated from cells (Figure 5, panels C−D). The polarized ROIs from liver and muscle tissue mitochondria exhibit mobility distributions that are decreased when compared to the distributions from the depolarized ROIs (Figure 6C). The Q−Q plot allows for

dx.doi.org/10.1021/ac403849x | Anal. Chem. 2014, 86, 4217−4226

comparisons of subtle differences between these distributions. For example, while the mobility distributions for polarized ROIs from both muscle and liver tissue are decreased, the difference in the distributions between polarized and depolarized ROIs from liver is more uniform than the distributions between polarized and depolarized ROIs from muscle (i.e., points for most percentiles are evenly spaced and fall away from the $y = x$ line). This reflects the broader range of the distributions of corrected mobility from liver mitochondria compared to muscle, which may reflect more heterogeneity in the surface composition of mitochondria from liver.

CONCLUSIONS

This report describes the first method to measure simultaneously membrane potential and electrophoretic mobility in individual, isolated mitochondria using the ratiometric dye JC-1. The use of CE-LIF provides the electrophoretic mobility of individual organelles, which is useful to investigate separations of mitochondrial subpopulations with different surface properties. The method is applicable to mitochondria isolated from cultured cells and from muscle and liver tissue. Highlighting the importance of individual mitochondrial analysis, the use of ROIs makes it possible to characterize polarized mitochondria in samples where depolarized mitochondria are present due to experimental factors that result in loss of membrane potential during preparation and analysis.

Analysis of ROIs revealed an effect of membrane potential on electrophoretic mobility: mitochondria in polarized ROIs had distributions of electrophoretic mobility that were more positive than those in depolarized ROIs, consistent with the capacitive model. This method could be used to investigate the effects of treatments to the mitochondrial surface (e.g., trypsin to cleave cytoskeletal proteins) to measure their relative contributions to mitochondrial mobility.[31] Different modes of separation could also be used; for example, this labeling scheme could be used with capillary isoelectric focusing to determine relationships between mitochondrial isoelectric point and membrane potential. Since the sample requirement is small and the method allows for analysis of membrane potential even if some mitochondria are disrupted during sample preparation, this method could even be applied to studies in which minimal amounts of samples are available (e.g., human tissue). Lastly, this work may enable future studies of the dependence of mitochondrial electrophoretic mobility on membrane potential and could aid in the design of separations of mitochondrial subpopulations with different surface properties, which may be important in aging and disease.

ASSOCIATED CONTENT

Supporting Information

Additional information as noted in text. This material is available free of charge via the Internet at http://pubs.acs.org.

AUTHOR INFORMATION

Corresponding Author

*E-mail: arriaga@umn.edu. Fax: 612-626-7541.

Notes

The authors declare no competing financial interest.

ACKNOWLEDGMENTS

This work was supported by the National Institutes of Health (Grant ROI-AG020866). G.G.W. was supported in part by a NIH Training Grant T32-AG029796.

REFERENCES

(1) Brand, M. D.; Nicholls, D. G. *Biochem. J.* **2011**, *435*, 297−312.
(2) Saraste, M. *Science* **1999**, *283*, 1488−1493.
(3) Huttemann, M.; Lee, I.; Pecinova, A.; Pecina, P.; Przyklenk, K.; Doan, J. W. *J. Bioenerg. Biomembr.* **2008**, *40*, 445−456.
(4) Twig, G.; Elorza, A.; Molina, A. J. A.; Mohamed, H.; Wikstrom, J. D.; Walzer, G.; Stiles, L.; Haigh, S. E.; Katz, S.; Las, G.; Alroy, J.; Wu, M.; Py, B. F.; Yuan, J.; Deeney, J. T.; Corkey, B. E.; Shirihai, O. S. *EMBO J.* **2008**, *27*, 433−446.
(5) Matsuda, N.; Sato, S.; Shiba, K.; Okatsu, K.; Saisho, K.; Gautier, C. A.; Sou, Y.; Saiki, S.; Kawajiri, S.; Sato, F.; Kimura, M.; Komatsu, M.; Hattori, N.; Tanaka, K. *J. Cell Biol.* **2010**, *189*, 211−221.
(6) Keil, V. C.; Funke, F.; Zeug, A.; Schild, D.; Muller, M. *Eur. J. Physiol.* **2011**, *462*, 693−708.
(7) Chen, H. C.; Chomyn, A.; Chan, D. C. *J. Biol. Chem.* **2005**, *280*, 26185−26192.
(8) Adhihetty, P. J.; Ljubicic, V.; Menzies, K. J.; Hood, D. A. *Am. J. Physiol.: Cell Physiol.* **2005**, *289*, C994−C1001.
(9) Navratil, M.; Terman, A.; Arriaga, E. A. *Exp. Cell Res.* **2008**, *314*, 164−172.
(10) Narendra, D.; Tanaka, A.; Suen, D. F.; Youle, R. J. *J. Cell Biol.* **2008**, *183*, 795−803.
(11) Picard, M.; Taivassalo, T.; Ritchie, D.; Wright, K. J.; Thomas, M. M.; Romestaing, C.; Hepple, R. T. *PLoS One* **2011**, *6*, e18317.
(12) Labajova, A.; Vojtiskova, A.; Krivakova, P.; Kofranek, J.; Drahota, Z.; Houstek, J. *Anal. Biochem.* **2006**, *353*, 37−42.
(13) Lim, T. S.; Davila, A.; Wallace, D. C.; Burke, P. *Lab Chip* **2010**, *10*, 1683−1688.
(14) Perry, S. W.; Norman, J. P.; Barbieri, J.; Brown, E. B.; Gelbard, H. A. *Biotechniques* **2011**, *50*, 98−115.
(15) Ehrenberg, B.; Montana, V.; Wei, M. D.; Wuskell, J. P.; Loew, L. M. *Biophys. J.* **1988**, *53*, 785−794.
(16) Smiley, S. T.; Reers, M.; Mottolahartshorn, C.; Lin, M.; Chen, A.; Smith, T. W.; Steele, G. D.; Chen, L. B. *Proc. Natl. Acad. Sci. U.S.A.* **1991**, *88*, 3671−3675.
(17) Reers, M.; Smith, T. W.; Chen, L. B. *Biochemistry* **1991**, *30*, 4480−4486.
(18) Salvioli, S.; Ardizzoni, A.; Franceschi, C.; Cossarizza, A. *FEBS Lett.* **1997**, *411*, 77−82.
(19) Plasek, J.; Sigler, K. *J. Photochem. Photobiol. B* **1996**, *33*, 101−124.
(20) Perry, S. W.; Norman, J. P.; Barbieri, J.; Brown, E. B.; Gelbard, H. A. *Biotechniques* **2011**, *50*, 98−115.
(21) Birkan, B.; Gulen, D.; Ozcelik, S. *J. Phys. Chem. B* **2006**, *110*, 10805−10813.
(22) Karaca, S.; Elmaci, N. *J. Mol. Struct.: Theochem* **2009**, *915*, 149−159.
(23) von Berlepsch, H.; Bottcher, C. *Langmuir* **2013**, *29*, 4948−4958.
(24) Scaduto, R. C.; Grotyohann, L. W. *Biophys. J.* **1999**, *76*, 469−477.
(25) Cossarizza, A.; Ceccarelli, D.; Masini, A. *Exp. Cell Res.* **1996**, *222*, 84−94.
(26) Zand, K.; Pham, T.; Davila, A.; Wallace, D. C.; Burke, P. J. *Anal. Chem.* **2013**, *85*, 6018−6025.
(27) Duffy, C. F.; Fuller, K. M.; Malvey, M. W.; O'Kennedy, R.; Arriaga, E. A. *Anal. Chem.* **2002**, *74*, 171−176.
(28) Moe, M. K.; Samuelsen, P. J.; Nielsen, H. V.; Nielsen, K. M. *Electrophoresis* **2010**, *31*, 1344−1349.
(29) Fuller, K. M.; Duffy, C. F.; Arriaga, E. A. *Electrophoresis* **2002**, *23*, 1571−1576.
(30) Zhao, W. F.; Waisum, O.; Fung, Y. S.; Cheung, M. P. *Eur. J. Lipid Sci. Technol.* **2010**, *112*, 1058−1066.
(31) Kostal, V.; Arriaga, E. A. *Anal. Chem.* **2011**, *83*, 1822−1829.

(32) Fuller, K. M.; Arriaga, E. A. *J. Chromatogr., B* **2004**, *806*, 151−159.
(33) Radko, S. P.; Chrambach, A. *Electrophoresis* **2002**, *23*, 1957−1972.
(34) Phayre, A. N.; Farfano, H. M. V.; Hayes, M. A. *Langmuir* **2002**, *18*, 6499−6503.
(35) Pysher, M. D.; Hayes, M. A. *Langmuir* **2004**, *20*, 4369−4375.
(36) Pysher, M. D.; Hayes, M. A. *Langmuir* **2005**, *21*, 3572−3577.
(37) Chen, Y.; Arriaga, E. A. *Langmuir* **2007**, *23*, 5584−5590.
(38) Kamo, N.; Muratsugu, M.; Kurihara, K.; Kobatake, Y. *FEBS Lett.* **1976**, *72*, 247−250.
(39) Aiuchi, T.; Kamo, N.; Kurihara, K.; Kobatake, Y. *Biochemistry* **1977**, *16*, 1626−1630.
(40) Tsoneva, I. C.; Tomov, T. C. *Bioelectrochem. Bioenerg.* **1984**, *12*, 253−258.
(41) Pressman, B. C. *Annu. Rev. Biochem.* **1976**, *45*, 501−530.
(42) Ramsay, L. M.; Dickerson, J. A.; Dada, O.; Dovichi, N. J. *Anal. Chem.* **2009**, *81*, 1741−1746.
(43) Herman, T. K.; Mackowiak, S. A.; Kaufman, L. J. *Rev. Sci. Instrum.* **2009**, *80*, 016107.
(44) Kostal, V.; Fonslow, B. R.; Arriaga, E. A.; Bowser, M. T. *Anal. Chem.* **2009**, *81*, 9267−9273.
(45) Frezza, C.; Cipolat, S.; Scorrano, L. *Nat. Protoc.* **2007**, *2*, 287−295.
(46) Poe, B. G.; Duffy, C. F.; Greminger, M. A.; Nelson, B. J.; Arriaga, E. A. *Anal. Bioanal. Chem.* **2010**, *397*, 3397−3407.
(47) Whiting, C. E.; Arriaga, E. A. *Electrophoresis* **2006**, *27*, 4523−4531.
(48) Shen, Y. F.; Smith, R. D. *J. Microcolumn Sep.* **2000**, *12*, 135−141.
(49) Wolken, G. G.; Kostal, V.; Arriaga, E. A. *Anal. Chem.* **2011**, *83*, 612−618.
(50) Duffy, C. F.; Gafoor, S.; Richards, D. P.; Admadzadeh, H.; O'Kennedy, R.; Arriaga, E. A. *Anal. Chem.* **2001**, *73*, 1855−1861.
(51) Davis, J. M.; Arriaga, E. A. *J. Chromatogr., A* **2009**, *1216*, 6335−6342.
(52) Davis, J. M.; Arriaga, E. A. *Anal. Chem.* **2010**, *82*, 307−315.
(53) Andreyev, D.; Arriaga, E. A. *Anal. Chem.* **2007**, *79*, 5474−5478.
(54) Whiting, C. E.; Arriaga, E. A. *J. Chromatogr., A* **2007**, *1157*, 446−453.
(55) Perelman, A.; Wachtel, C.; Cohen, M.; Haupt, S.; Shapiro, H.; Tzur, A. *Cell Death Dis.* **2012**, *3*, e430.
(56) Saunders, J. E.; Beeson, C. C.; Schnellmann, R. G. *J. Bioenerg. Biomembr.* **2013**, *45*, 87−99.
(57) Benz, R. *Biochim. Biophys. Acta* **1994**, *1197*, 167−196.